

Model of accelerated carcinogenesis based on proliferative stress and inflammation for doses relevant to radiotherapy

Uwe Schneider · Brigitte Schäfer

Received: 28 March 2012 / Accepted: 31 July 2012 / Published online: 17 August 2012
© Springer-Verlag 2012

Abstract Recent findings demonstrate that accelerated carcinogenesis following liver regeneration is associated with chronic inflammation-induced double-strand DNA breaks in cells, which escaped apoptosis due to proliferative stress. In this work, proliferative stress and inflammation-based carcinogenesis at large dose were included in a cancer induction model considering fractionation. At large dose, tissue injury due to irradiation could be so severe that under the regenerative proliferative stress induced by cell loss, the genomic unstable cells generated during irradiation and/or inflammation escape senescence or apoptosis and reenter the cell cycle, triggering enhanced carcinogenesis. This acceleration—modeled to be proportional to the number of repopulated cells—is only significant, however, when tissue injury is severe and thus proportional to the cell loss in the tissue. The general solutions to the resulting differential equations for carcinoma induction were computed. In case of full repopulation or acute low-dose irradiation, the acceleration term disappears from the equation describing cancer induction. The acceleration term is affecting the dose–response curve for carcinogenesis only at large doses. An example for bladder cancer is shown. An existing model for cancer

induction after fractionated radiotherapy which is based on cell mutations was extended here by including the effects of inflammation and proliferative stress, and an additional model parameter was established which describes acceleration. The new acceleration parameter affects the dose–response model only at large dose and is only effective when the tissue is not capable of fully repopulating between dose fractions.

Keywords Carcinogenesis · Modeling · Inflammation · Proliferative stress

Introduction

Over the past three decades, advances in cancer treatment have steadily improved survival times. As a consequence, among all cancer survivors in 2001, 14 % had received a cancer diagnosis more than 20 years ago (Rowland et al. 2004). Approximately half of these long-term survivors received a radiotherapy treatment and are thus subject to radiation-related side effects. These long-term survivors experience a significant incidence of chronic health problems after their treatment, including second primary cancer (Suit et al. 2007).

Research and development in radiation oncology is mainly directed to further increase the cure rates. This is currently achieved by application of new radiation treatment modalities such as intensity-modulated radiotherapy (IMRT), intensity-modulated arc-therapy and proton and heavy-ion radiotherapy. Note, however, that the long-term risks from modern radiotherapy treatment techniques have not yet been determined and are unlikely to become apparent for many years, due to the long latency time for solid tumor induction. Therefore, decisions on potential

U. Schneider
Radiotherapy Hirslanden AG, Institute for Radiotherapy,
Rain 34, 5001 Aarau, Switzerland

U. Schneider (✉)
Vetsuisse Facutly, University of Zürich, Winterthurerstrasse 260,
8057 Zurich, Switzerland
e-mail: uschneider@vetclinics.uzh.ch

B. Schäfer
Department of Internal Medicine, Kantonsspital Baden,
Baden, Switzerland

risk induction must be made using theoretical predictions (Newhauser and Durante 2011) including the development of models for risk assessment based on the current knowledge of radiation-induced carcinogenesis.

Several models for risk assessment have been proposed. Since dose fractionation is common in radiation therapy and can be important for carcinogenesis, it was included in recent models by considering cell repopulation between the dose fractions (Sachs and Brenner 2005; Shuryak et al. 2009a; Shuryak et al. 2009b; Pfaffenberger et al. 2009; Schneider 2009; Schneider et al. 2011). Repopulation tends to counteract cell killing and accounts for large discrepancies between the standard model for cancer induction neglecting fractionation at high doses (“bell-shaped model”) and recent second cancer data (Hall 2000).

Practically, all models describe carcinogenesis induced by ionizing radiation as a (multi-)mutational process in the cells. This approach to cancer induction might work well at low doses. At large doses (>20 Gy), however, also cell sterilization effects can play an important role. Sterilization of a large number of cells could lead, for example, to inflammations (Philip et al. 2004) or proliferative stress (Barash et al. 2010), which additionally could initiate carcinogenesis. Thus, cancer induction at large dose could be systematically underestimated by current models.

The aim of the present study was to include the mechanisms of proliferative stress and inflammation-based carcinogenesis at large dose into a cancer induction model including fractionation. This was accomplished by applying recent results of Barash et al. (2010), who found that accelerated carcinogenesis following liver regeneration is associated with chronic inflammation-induced double-strand DNA breaks in cells that escaped apoptosis due to proliferative stress.

Materials and methods

Accelerated carcinogenesis following organ regeneration

Barash et al. (2010) reported in a recent publication that liver resection significantly promotes carcinogenesis and attenuates regeneration. They proposed that under the regenerative proliferative stress induced by liver resection, the genomic unstable hepatocytes generated during chronic inflammation escape senescence or apoptosis and reenter the cell cycle, triggering the enhanced carcinogenesis. In their study Mdr2-KO mice, a model of inflammation-associated cancer, underwent partial hepatectomy, which led to enhanced hepatocarcinogenesis. Barash et al. (2010) clarified the immediate and long-term contributions of the DNA damage response to hepatocellular carcinoma development and recurrence.

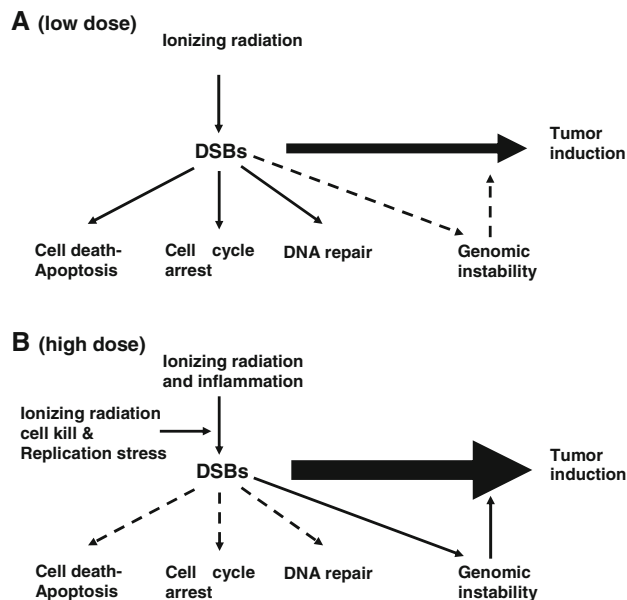


Fig. 1 **a** Situation at low-dose ionizing radiation where inflammatory processes are negligible; ionizing radiation is inducing double-strand breaks; however, apoptosis, cell cycle arrest and DNA repair are actively eliminating mutated cells. **b** Large dose of ionizing radiation is responsible for massive tissue injury, triggering enhanced cell proliferation; the cells generated during irradiation and inflammation may escape senescence and apoptosis and reenter the cell cycle, thus triggering enhanced carcinogenesis

In the present work, it is proposed that this mechanism also plays a role in radiotherapy where large doses of ionizing radiation affect healthy organs adjacent to the target volume. Inaccurate DNA repair can lead to mutations and/or chromosomal aberrations that can contribute to carcinogenesis (Bartkova et al. 2005; Van Gent et al. 2001). Proliferative stress during radiotherapy is triggered by the sterilization of large parts of an organ by radiation and the following regeneration of the lost cells (Dörr and Kummermehr 1990). Some of the cells created during regeneration are genomic unstable, due to radiation-induced DNA damage or inflammatory processes (as a consequence of high-dose radiation therapy). Some of these genomic unstable cells may escape senescence and apoptosis under the regenerative proliferative stress, reenter the cell cycle and thus trigger enhanced carcinogenesis. This mechanism is drafted in Fig. 1.

Mathematical formulation of accelerated carcinogenesis following organ regeneration

In the following a model is developed which is close to a mechanistic model for predicting cancer induction after fractionated radiotherapy (Schneider 2009). Cell kill is described by a linear-quadratic dose–response model, while cancer induction is, for each dose fraction, modeled

linearly with dose, and between the dose fractions, repopulation is allowed.

It is assumed that the tissue or organ of interest consists of N_0 cells before it is irradiated. At this stage there is no distinction between cells that represent a particular function and do not divide, and stem cells that are dividing. The tissue is then irradiated with a fractionated treatment schedule of equal-dose fractions d_f up to a dose D . It is important to note here that the single-dose fraction d_f should not exceed a dose where the linear-no-threshold hypothesis is no more valid, that is, d_f should be lower than 2 or 3 Gy.

The number of original cells after irradiation is reduced by cell kill. A number of N cells survive one-dose fraction (Eq. 1).

$$\frac{dN(D)}{dD} = -\alpha'N(D), \tag{1}$$

where the cell kill parameter α' is for fractionated treatment taken as

$$\alpha' = \alpha + \beta d_f \tag{2}$$

where α and β are the usual parameters from the linear-quadratic model for the tissues of interest.

It is further assumed that the number of killed original tissue cells $N_0 - N$ is replaced by a number of new cells R with a repopulation rate that is proportional to cell loss $N_0 - N - R$. This is modeled by:

$$\frac{dR(D)}{dD} = -\alpha'R(D) + \alpha' \frac{r}{1-r} (N_0 - N(D) - R(D)), \tag{3}$$

$\forall r \in]0, 1[$

where the parameter r is chosen such that it is proportional to the ability of the tissue to repopulate; this parameter varies between 0 for no and 1 for full repopulation between single-dose fractions.

Here, it is assumed that the repopulation kinetics of repopulated cells follows the same basic patterns as that of normal cells.

Cells that were irradiated can be mutated and have the potential to develop a tumor. In the context of the present work, the word “mutation” is used as a synonym for each cell transformation, which results in a new tumor cell. In fact, the development of a tumor usually implies several mutations. The mutational process is modeled to be proportional to the number of cells $(N + R)$ present at the time of irradiation. The proportionality constant is μ .

At large dose, tissue injury due to irradiation could be so severe that under the regenerative proliferative stress induced by cell loss, the genomic unstable cells generated during irradiation and/or inflammation may escape senescence or apoptosis and reenter the cell cycle, triggering enhanced carcinogenesis. This acceleration must be proportional (ρ) to

the number of repopulated cells R . However, acceleration is only significant when tissue injury is severe and thus proportional to $(1 - (N - R)/N_0)$, which characterizes the amplitude of tissue injury. The differential equation describing carcinoma induction is then:

$$\frac{dM_C(D)}{dD} = -\alpha'M_C(D) + \mu(N(D) + R(D)) + \rho R(D) \left(1 - \frac{N(D) - R(D)}{N_0}\right) \tag{4}$$

where M_C is the number of mutated cells that lead to carcinoma induction. It is assumed here that the same cell kill parameter α' applies to normal, repopulated and mutated cells. For carcinoma induction, it is further assumed that the original tissue before irradiation consists, among others, of dividing cells, and therefore, the induction rate is proportional to the sum of the number of surviving original and repopulated cells.

Cancer risk in this simple model is defined as the ratio of the number of mutated cells to the number of original cells in the tissue. This was done since we believe that an observed cancer rate in an organ should be more or less independent of the organ’s volume or mass. This hypothesis is supported by the fact that various cell sterilization mechanisms are cell-specific (i.e., apoptosis, senescence) or also scale with organ size (i.e., the power of the immune system).

Results

Equations 1, 3 and 4 are first-order non-homogeneous linear differential equations that can be solved analytically using the initial conditions that the number of original cells $N(0)$ before treatment is N_0 and the number of repopulating cells $R(0)$ and mutated cells $M_c(0)$ is zero before the onset of radiation. The problem is then solved by

$$N(D) = N_0 e^{-\alpha'D} \tag{5}$$

$$R(D) = N_0 \left\{ r + (1-r) \frac{e^{\alpha'D}}{e^{\alpha'D}} - e^{-\alpha'D} \right\} \tag{6}$$

$$M_C(D) = \frac{N_0 e^{-\alpha'D}}{\alpha' r (r+1)} \left\{ -\rho r (r-1)^3 e^{\frac{\alpha'D(r+1)}{(r-1)}} - (r+1)(r-1)^2 (\mu + \rho - 2\rho r) e^{\frac{\alpha'D}{(r-1)}} - \rho r (r+1)(r-1)^2 e^{\frac{\alpha'D}{(r-1)}} + r^2 (r+1) \times (\mu + \rho - \rho r) e^{\alpha'D} + \rho r^4 + \rho r^3 (\alpha'D - 1) + 2r^2 (\rho - \mu) - r(\mu + 3\rho + \rho \alpha'D) + \mu + \rho \right\}, \tag{7}$$

$\forall r \in]0, 1[$

As described above, excess absolute risk (EAR) is then simply M_c/N_0 .

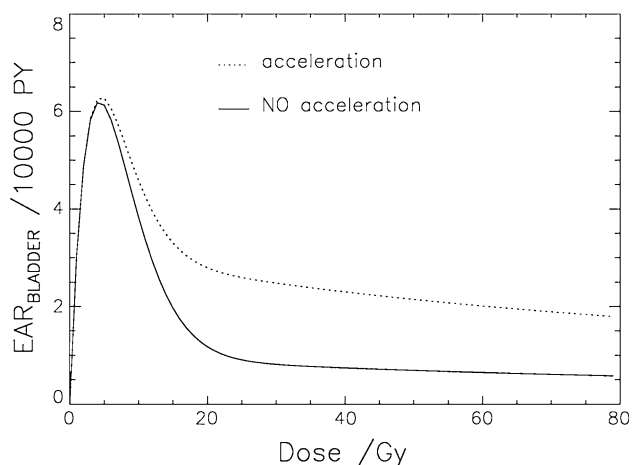


Fig. 2 Dose–response relationship for bladder cancer as a function of point dose in the organ. The *solid line* represents a fit to Hodgkin’s data with bladder doses lower than 15 Gy, obtained by a model without acceleration. In contrast, the *dotted line* represents the dose–response relationship including acceleration as calculated in this work

Due to the findings of Barash et al. (2010), the induction of liver cancer is one example where accelerated carcinogenesis could be of importance. We hypothesize that this model can also be of importance for other locations. A typical clinical example is bladder cancer, which can be a side effect of treating prostate patients with high dose of radiation. Since the bladder is located close to the target volume (prostate), it can receive dose in the order of 70 Gy. At such large doses, tissue injury and cell loss due to irradiation could be so severe that the genomic unstable cells generated during irradiation may escape senescence or apoptosis and trigger enhanced carcinogenesis. An evidence that acceleration might be important for the induction of bladder cancer is the fact that a bladder dose–response model that was fitted to low-dose data ($D_{\text{Bladder}} < 15$ Gy) from Hodgkin’s patients (Schneider and Walsh 2008; Schneider et al. 2011) is underestimating risk when applied to patients who were treated for prostate carcinoma ($50 \text{ Gy} < D_{\text{Bladder}} < 70$ Gy). The dose–response relationship for bladder cancer which was fitted to Hodgkin’s patients is plotted as the solid line in Fig. 2. The corresponding fitting parameters were $\mu = 3.8/10,000$ PY/Gy, $\alpha = 0.219/\text{Gy}$, $R = 0.09$ and $\rho = 0/10,000$ PY/Gy, respectively (Schneider et al. 2011). If this is applied to dose distributions from historical prostate radiotherapy treatments, an EAR of 3 cases per 10,000 PY is obtained. This is in contradiction to epidemiological studies (Brenner et al. 2000) where 9 cases per 10,000 PY were found. If an acceleration parameter of $\rho = 8/10,000$ PY/Gy is used in Eq. 7, which is shown as the dotted line in Fig. 2, then the epidemiological findings can be reproduced.

In Fig. 3 the acceleration is shown as a function of the repopulation factor for four different ρ values for liver

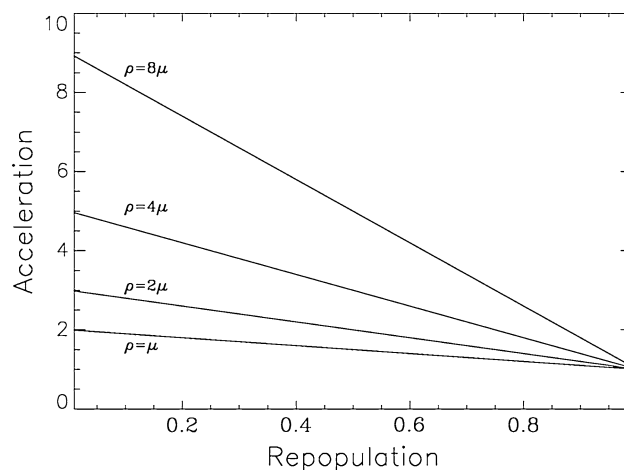


Fig. 3 Acceleration for liver cancer as a function of the repopulation factor, for four different ρ values. Acceleration is here defined as the maximum ratio of EAR including acceleration to that without acceleration for a dose range up to 50 Gy

cancer. Acceleration is here defined as the maximum ratio of EAR including acceleration to EAR without acceleration, for a dose range up to 50 Gy.

Discussion

Equation 3 describes the repopulation rate for tissues that correspond to a repopulation strength between no and full repopulation ($0 < r < 1$). One question is what is happening for zero and full repopulation.

If there is no repopulation in the tissue, there are no repopulated cells, and thus, $R(d)$ is always zero. If we use $R(d) = 0$, then from Eq. 4 it follows

$$M_C(D, r \rightarrow 0) = \mu N_0 D e^{-\alpha D}. \quad (8)$$

In this limit, cancer risk is solely proportional to μ and independent of ρ , which is consistent with the assumption that for acute exposures carcinogenesis is triggered mainly by mutational processes. If Eq. 8 is taken in the limit of small dose (i.e., for $\alpha D \ll 1$), our model is in perfect agreement with the linear-no-threshold model if excess absolute cancer risk is expressed by M_C/N_0 :

$$\begin{aligned} \text{EAR}_C(D, r \rightarrow 0) &= \frac{M_C(D, r \rightarrow 0)}{N_0} \approx \mu D \cdot (1 - \alpha D) \\ &\approx \mu D \quad \text{for } \alpha D \ll 1 \end{aligned} \quad (9)$$

Hence, in Eq. 7 the parameter μ represents the initial slope at low dose and may be obtained directly from the analysis of the A-bomb survivors (Preston et al. 2007; Schneider et al. 2011). Usually, when Eq. 7 is fitted, a variation of the parameter μ is allowed in the 95 % confidence interval of the A-bomb survivor data.

In case of full repopulation ($r = 1$) between dose fractions, Eq. 3 is redundant, since the number of repopulated cells is simply

$$R(D) = N_0 - N = N_0(1 - e^{-\alpha'D}) \quad (10)$$

When Eqs. 1, 10 and 4 are solved, EAR for carcinoma induction is:

$$\text{EAR}_C(D, r \rightarrow 1) = \frac{\mu_C}{\alpha'}(1 - e^{-\alpha'D}), \quad (11)$$

In case of full repopulation, sterilized cells are fully replaced after each fraction, and thus, no proliferative stress can occur. As a consequence, EAR is independent of ρ . This is also shown in Fig. 3 where the accelerated carcinogenesis is, independent of the parameter ρ , negligible at full repopulation between the dose fractions, and the value of the acceleration becomes unity. However, repopulation power decreases as acceleration becomes more important, since some of the cells created during repopulation are genomic unstable (due to proliferative stress) and can escape senescence and apoptosis.

It should be noted here that in addition to the limitations of the model without acceleration, which is in detail discussed by Schneider (2009), the acceleration introduced in the present study was modeled solely as a function of dose during treatment, and thus, time-related effects independent of dose such as the delayed start of repopulation (Dörr and Kummermehr 1990) were completely neglected.

Note that proliferative stress might be only one mechanism that can lead to accelerated mutagenesis. Contributions to further mutagenesis might include enhanced tissue hypoxia developing years after irradiation because of late vascular effects.

One important question is for which organs the model can be applied. Proliferative stress is important when the repopulation power of the tissue is small (see Fig. 3). In a recent publication (Schneider et al. 2011) the model without acceleration was fitted to second cancer data, and the parameter r was obtained. Organs that correspond to r smaller than 0.3 comprise female breast, small intestine, liver, bladder and salivary gland.

Conclusion

In the present study, an existing model for cancer induction after fractionated radiotherapy which is based on cell mutations was extended by including the effects of inflammation and proliferative stress. It is proposed that tissue injury due to high doses of radiation may be due to enhanced cell proliferation. The cells generated during irradiation and inflammation can escape senescence and

apoptosis and reenter the cell cycle, thus triggering an enhanced carcinogenesis. An additional model parameter ρ was introduced into the model to describe this acceleration. The new acceleration parameter affects the dose–response model only at large dose and is only effective when the tissue is not capable of fully repopulating between dose fractions.

The repopulation power of the different tissues suggests that acceleration might be important for female breast, small intestine, liver, bladder and salivary gland. However, more research work is necessary to analyze the impact of accelerated carcinogenesis for radiotherapy patients. In particular, detailed observations of second cancer induction rates after radiotherapy at different dose levels are necessary.

References

- Barash HR, Gross E, Edrei Y, Ella E, Israel A, Cohen I, Corchia N, Ben-Moshe T, Pappo O, Pikarsky E, Goldenberg D, Shiloh Y, Galun E, Abramovitch R (2010) Accelerated carcinogenesis following liver regeneration is associated with chronic inflammation-induced double-strand DNA breaks. *Proc Natl Acad Sci USA* 107(5):2207–2212
- Bartkova J, Horejsí Z, Koed K, Krämer A, Tort F, Zieger K, Gulberg P, Sehested M, Nesland JM, Lukas C, Ørntoft T, Lukas J, Bartek J (2005) DNA damage response as a candidate anti-cancer barrier in early human tumorigenesis. *Nature* 434:864–870
- Brenner DJ, Curtis RE, Hall EJ, Ron E (2000) Second malignancies in prostate carcinoma patients after radiotherapy compared with surgery. *Cancer* 88(2):398–406
- Dörr W, Kummermehr J (1990) Accelerated repopulation of mouse tongue epithelium during fractionated irradiations or following single doses. *Radiother Oncol* 17(3):249–259
- Hall EJ (2000) Radiation, the two-edged sword: cancer risks at high and low doses. *Cancer J* 6:343–350
- Newhauser WD, Durante M (2011) Assessing the risk of second malignancies after modern radiotherapy. *Nat Rev Cancer* 11:38–448
- Pfaffenberger A, Schneider U, Poppe B, Oelfke U (2009) Phenomenological modelling of second cancer incidence for radiation treatment planning. *Z Med Phys* 19(4):236–250
- Philip M, Rowley DA, Schreiber H (2004) Inflammation as a tumor promoter in cancer induction. *Semin Cancer Biol* 14(6):433–439
- Preston DL, Ron E, Tokuoka S, Funamoto S, Nishi N, Soda M, Mabuchi K, Kodama K (2007) Solid cancer incidence in atomic bomb survivors: 1958–1998. *Radiat Res* 168(1):1–64
- Rowland J, Mariotto A, Aziz N, Tesaro G, Feuer EJ (2004) Cancer survivorship—United States, 1971–2001. *MMWR Morb Mortal Wkly Rep* 53:526–529
- Sachs RK, Brenner DJ (2005) Solid tumor risks after high doses of ionizing radiation. *Proc Natl Acad Sci USA* 102:13040–13045
- Schneider U (2009) Mechanistic model of radiation-induced cancer after fractionated radiotherapy using the linear-quadratic formula. *Med Phys* 36:1138–1143
- Schneider U, Walsh L (2008) Cancer risk estimates from the combined Japanese A-bomb and Hodgkin cohorts for doses relevant to radiotherapy. *Radiat Environ Biophys* 47(2):253–263
- Schneider U, Sumila M, Robotka J (2011) Site-specific dose–response relationships for cancer induction from the combined Japanese

- A-bomb and Hodgkin cohorts for doses relevant to radiotherapy. *Theor Biol Med Model* 8:27
- Shuryak I, Hahnfeldt P, Hlatky L, Sachs RK, Brenner DJ (2009a) A new view of radiation-induced cancer: integrating short- and long-term processes. Part I: approach *Radiat Environ Biophys* 48: 263–274; Erratum (2011) *Radiat Environ Biophys* 50: 607–608
- Shuryak I, Hahnfeldt P, Hlatky L, Sachs RK, Brenner DJ (2009b) A new view of radiation-induced cancer: integrating short- and long-term processes. Part II: second cancer risk estimation *Radiat Environ Biophys* 48: 275–286; Erratum (2011) *Radiat Environ Biophys* 50: 607–608
- Suit H, Goldberg S, Niemierko A, Ancukiewicz M, Hall E, Goitein M, Wong W, Paganetti H (2007) Secondary carcinogenesis in patients treated with radiation: A review of data on radiation-induced cancers in human, non-human primate, canine and rodent subjects *Radiat Res* 167: 12–42; Erratum. 2007. *Radiat Res* 167: 748
- Van Gent DC, Hoeijmakers JHJ, Kanaar R (2001) Chromosomal stability and the DNA double-stranded break connection. *Nat Rev Genet* 2:196–206